Responsivity enhancement of a Strained Silicon Field Effect Transistor detector at 0.3 THz using the terajet effect

I. V. Minin,[1] O. V. Minin,[1] J.Salvador-Sánchez,[2] J.A. Delgado-Notario,[2,3] J. Calvo-Gallego,[2] M. Ferrando-Bataller,[4] K. Fobelets,[5] J.E. Velázquez-Pérez,[2] and Y. M. Meziani[2, a)]

[1)]*Tomsk Polytechnical University, 30 Lenin Avenue, Tomsk, 634050, Russia*

[2)]*Nanotech Group, Salamanca University, Facultad de Ciencias. Plaza de la Merced, s/n. Edificio Trilingüe, 37008, Salamanca, Spain*

[3)]*CENTERA Laboratories, Institute of High Pressure Physics, Polish Academy of Sciences, 29/37 Sokołowska Str, Warsaw, Poland*

[4)]*Departament of Communications, Telecommunication Engineering School, Universitat Politècnica de València, 46022, Valencia, Spain*

[5)]*Department of Electrical and Electronic Engineering, Imperial College, South Kensington Campus, London SW7 2AZ, UK*

(Dated: 17 November 2021)

We report on the enhancement of the responsivity by more than one order of magnitude of a Silicon-based sub-THz detector when a mesoscopic dielectric particle was used to localize incident radiation to a sub-wavelength volume and focus it directly onto the detector. A strained-silicon Modulation Field Effect Transistor (Si-MODFET) was used as a direct detector on an incident terahertz beam at 0.3 THz. A systematic study in which Teflon cubes were placed in front of the detector to focus the terahertz beam was performed. In this study, cubes with different sizes were investigated and an enhancement of the responsivity up to 11 dB was observed for a cube with an edge length of 3.45 mm (or 3.45λ). Electromagnetic simulation results were in good agreement with the experimental ones and demonstrate that the size of the mesoscopic particle plays an important role to focalize the electric field within an area below the diffraction limit. This approach provides an efficient, uncostly and easy to implement method to substantially improve the responsivity and the noise equivalent power (NEP) of sub-THz detectors.

[a)]meziani@usal.es

I. INTRODUCTION

The Terahertz (THz) region is located between the infrared region and the RF/microwaves one and is commonly referred as the Terahertz gap[1] due to lack of sources and detectors in this spectral region. It's the bridging region between the Electronics (limited by the cutoff frequency of transistors) and Photonics (limited by the low energy). The broad range of potential applications of THz radiation has impulsed the research on THz components (emitters, detectors, modulators, etc.) to the point that new THz systems are already exploited in real-world applications[2–6]. The progress in new semiconductor materials and devices has fostered the research of room-temperature Terahertz detectors[7–9]. One of the major challenges for the development of THz detectors is the efficient coupling of the incoming electromagnetic (EM) radiation as the beam area is usually larger than the transistors used as detectors with active areas of hundreds of square-microns. In order to obtain a good coupling different approaches are used: antennas are attached to the device contacts, silicon lenses are placed close to the chip to focus the beam on the detector, arrays of detectors, etc.[10–13]. However, those methods are costly and complex to implement. Recently, in order to efficiently improve the coupling of the EM radiation and, hence, to increase the sensitivity of terahertz detectors[14–18], we introduced the use of the terajet effect. The terajet effect[19–22] provides a simple method to significantly improve the focusing of the terahertz beam by simply placing a low-loss dielectric particle with wavelength-scaled dimensions in front of the focal volume[23]. This makes possible to localize the radiation incident on the detector to sub-wavelength volumes and, thus, to overcome diffraction limitations, matching the size of the field localization region and the size of the sensitive part of both the field-effect transistor (FET) and point-contact detectors[24,25]. However, a systematic study is still necessary to further investigate the optimization of the THz detection by FET detectors using the terajet effect. To this aim we have designed and fabricated a set of mesoscopic particles (Polytetrafluoroethylene (PTFE)/Teflon cubes)[26,27] with different sizes that has been used to characterize the sub-THz response of a strained-Si MODFET detector under illumination at 0.3 THz in conditions under which the terajet effect takes place. The experimental results presented in this letter show a gain of around 11 dB when a cube with an edge size of 3.45mm (3.45λ, where λ is the wavelength of illuminating wave) was placed in the focal position in front of the detector.

II. METHODS

A strained-Si MODFET[28] was used for the detection of the incident terahertz radiation. The detector response is based on the damped oscillations of plasmons in the channel of the transistor[29]. The nonlinear properties of the two-dimensional (2D) electron plasma in the channel of the FET are at the origin of the THz detection in bands beyond the cut-off frequency of the transistor. This is one of the most promising ways to achieve direct detection of THz beams using solid-state devices at room temperature. This type of transistor could be easily integrated to mainstream Silicon technology and it has been intensively investigated as THz detector showing good responsivity, room temperature operation, fast response, low cost and low noise equivalent power[30,31]. More information of the device and its terahertz characterization can be found in ref.[31]. Figure 1 shows the schematic description and photos of the terahertz detection setup. The electronic terahertz source used in measurements is based on a dielectric resonator oscillator with a multiplication chain starting at the fundamental frequency of 12.5 GHz and emitting at 0.3 THz. An emitted power of 6 mW was measured by a calibrated detector close to the output of the source. The THz beam was collimated and focused by off-axis gold coated parabolic and planar mirrors and a Teflon based cube. A visible red LED in combination with an indium tin oxide (ITO) mirror[32] was used for the alignment of the THz beam (Figure 1-(a)&(c)). The size of this transistor including the contact pads is considerably smaller ($\sim$ 0.047 mm^2) than the terahertz beam at 0.3 THz ($\sim$ 7 mm^2). In order to enhance the coupling efficiency, a mesoscopic particle (a Teflon cube) was placed in front of the device at the focusing point. This produces the terajet effect as demonstrated by Minin et al.[24]. The size of the cube was designed in two different sets accordingly to the theory of antennas[33]. The first one of a size proportional to the wavelength with its edge size L given by: $L = (n \times 0.25) + \lambda$ where n=0,1,2,$\cdots$ and λ = 1mm (f=300GHz). For the second set, the propagation of the radiation inside the cube was taken into account and the wavelength was reduced by a factor $\sqrt{\varepsilon_r}$, where ε_r is the dielectric constant of the Teflon (~ 2.1). The size of the cube is given by $L = \lambda' + n \times \lambda'/2$ where $\lambda' = \lambda/\sqrt{\varepsilon_r}$. The cubes were fabricated using a CNC machine on a Teflon base where the distance between adjacent cubes was fixed at 10 mm to avoid any interference with the THz beam (**Refer to figures 1 & 2 of the Supplement Materials**).

The photo-induced drain-to-source voltage ΔU under THz illumination was measured using the lock-in technique where the THz beam was chopped at 298 Hz. The 0.3 THz beam spot with a radius of about 1.5 mm was centered within the cube. The two sets of Teflon's cubes with a base

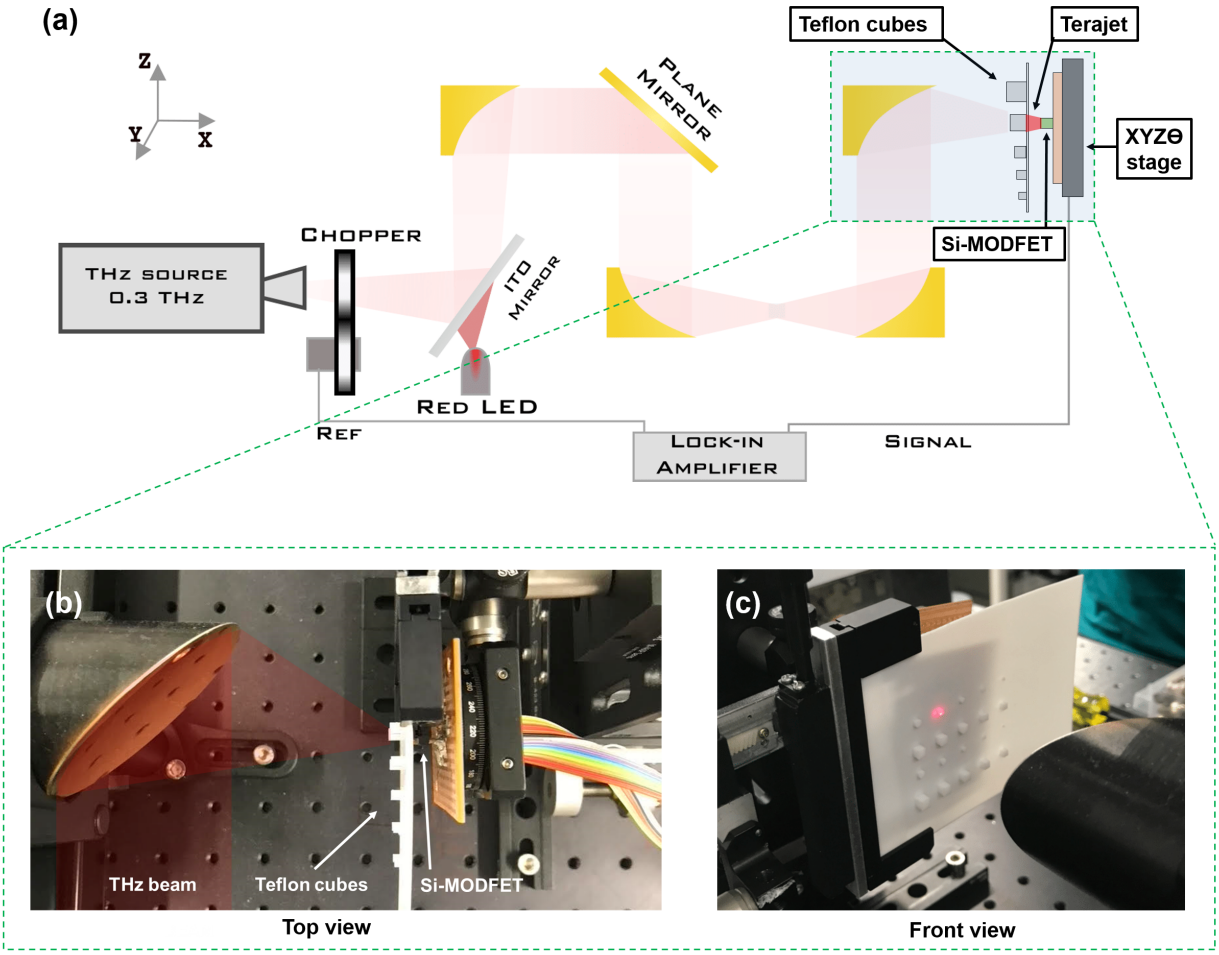

FIG. 1. (a) Schematic description of the Terahertz setup, (b) Top view at the second focal point of the setup showing the parabolic mirror that focuses the THz beam into the Teflon cube and generates the terajet focus on the Si-MODFET detector and (c) View of the sets of CNC micromachined cubes on the base of the Teflon Cubes along with the red LED used for alignment purposes.

of 1 mm of thickness were placed on an XYZ stage in front of the detector (Figure 1(b)-(c)).

The Responsivity ($\Re$) was extracted from the measured ΔU signal using the following equation:

$$\Re = \frac{\pi}{\sqrt{2}} \frac{\Delta U}{P} \frac{S_t}{S_a} \tag{1}$$

where P is the THz power incident on the transistor (P $\sim$1 mW was measured at the detector position by a calibrated pyroelectric detector). The factor $\pi/\sqrt{2}$ comes from the Fourier transform of the square-wave modulated THz signal detected as its rms value by the lock-in amplifier. S_t denotes the THz beam area given by $S_t = \pi r^2$ where $r = 1.5$ mm is the radius of the beam spot at 0.3 THz. S_a is the active area of the detector that was replaced by the diffraction limit area

$S_\lambda = \lambda^2/4$ in Eq. 1. The other key parameter is the Noise Equivalent Power (NEP)[34,35]; it was calculated using the detector responsivity and the following formula[24]:

$$NEP = \frac{N}{\Re} \tag{2}$$

where N is the noise spectral density of the transistor in $\mathrm{V}\cdot\sqrt{\mathrm{Hz}}$ given by $N = \sqrt{4k_BT\mathrm{R_{SD}}}$ where T is temperature in K, k_B the Boltzmann constant and $\mathrm{R_{SD}}$ the channel resistance. The channel resistance $\mathrm{R_{SD}}$ was extracted from the measured transfer characteristics of the transistor at a very low value of drain-to-source voltage, $\mathrm{V_{DS}}$=0.1V (**See figure 3 of the Supplement Materials**).

III. RESULTS AND DISCUSSIONS

Figure 2-(a) shows the obtained responsivity of the device under terahertz excitation at 0.3 THz. A clear enhancement of the responsivity was observed when a Teflon based cube was introduced. The measured responsivity when no cube was used was $\sim$ 20 V/W and reaches up to $\sim$ 74V/W when a cube with a dimension equal to 3.45 λ was placed at the focus of the terahertz beam in front of the detector (Fig. 1). As a consequence, the minimum NEP has been reduced by a factor of 3.6 from $\sim$260 pW/$\sqrt{Hz}$ with no cube down to $\sim$ 72 pW/$\sqrt{Hz}$ when a cube with L=3.45λ was introduced (Fig.2-(b)). This clearly demonstrates the enhancement of the response of the device due to the terajet effect [24]. To better analyze the results, we calculated the gain obtained using each cube with the formula: $\mathrm{Gain(dB)} = 20 \times \log\left[\Re_{Cube}/\Re_{NoCube}\right]$, where $\Re_{Cube}$ and $\Re_{NoCube}$ are the maximum responsivity with and without the cube, respectively. Figure 3 shows the obtained gain as a function of the size of the cube. A maximum of gain close to 11 dB was obtained by using the cube with L = 3.45 mm.

In order to understand the experimental results, full-wave electromagnetic simulations were performed using the software CST[36]. In this study, the Maxwell equations were solved without any simplifying assumption in both sets of Teflon cubes take into account the base as shown in Fig.1-(c). It's a standard method to analyze electrically large structures where the physical size is much larger than the wavelength. The impinging terahertz beam was modeled as a plane wave propagating along the z direction with a linear polarization along the x direction. The magnitude of the incident electric field was fixed at $E_x = 1$ V/m. The cube streches from z=-L to z=0 and the base between z=0 and z=1mm. The mesh size was defined by the CST simulator and depends on the size of the cube. For example, for the cube with L=3.45mm, the smallest and largest cells

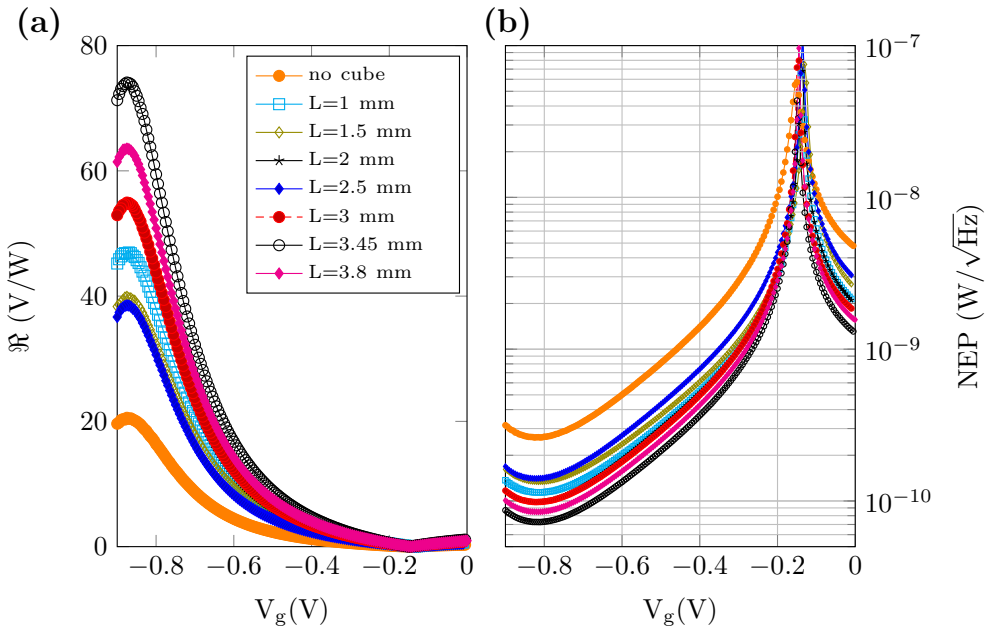

FIG. 2. (a) Responsivity of the device under excitation at 0.3THz versus the gate voltage. (b) The NEP extracted from Eq. (2)

.

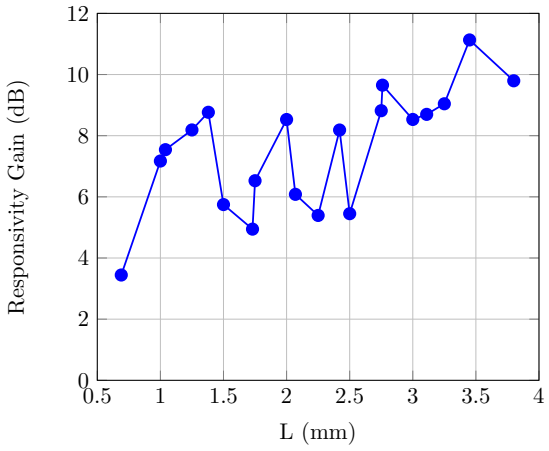

FIG. 3. Responsivity gain in dB as a function of the cube size.

were 0.0247984 and 0.0568182 mm, respectively. Figure 4 shows the intensity of the electric field for the case of two cubes with L=2.42mm and L=3.45mm. As can be seen in the figure the introduction of a cube induces the formation of an area in which the electric field is concentrated as a result of the terajet beam effect. It can be observed that the position of the maximum (the focal distance) of the electric field intensity depends on the cube size[19]. The focal distance of the terajet

is defined as the distance from the shadow surface of the base to the point where the maximum of field intensity inside the terajet is reached.

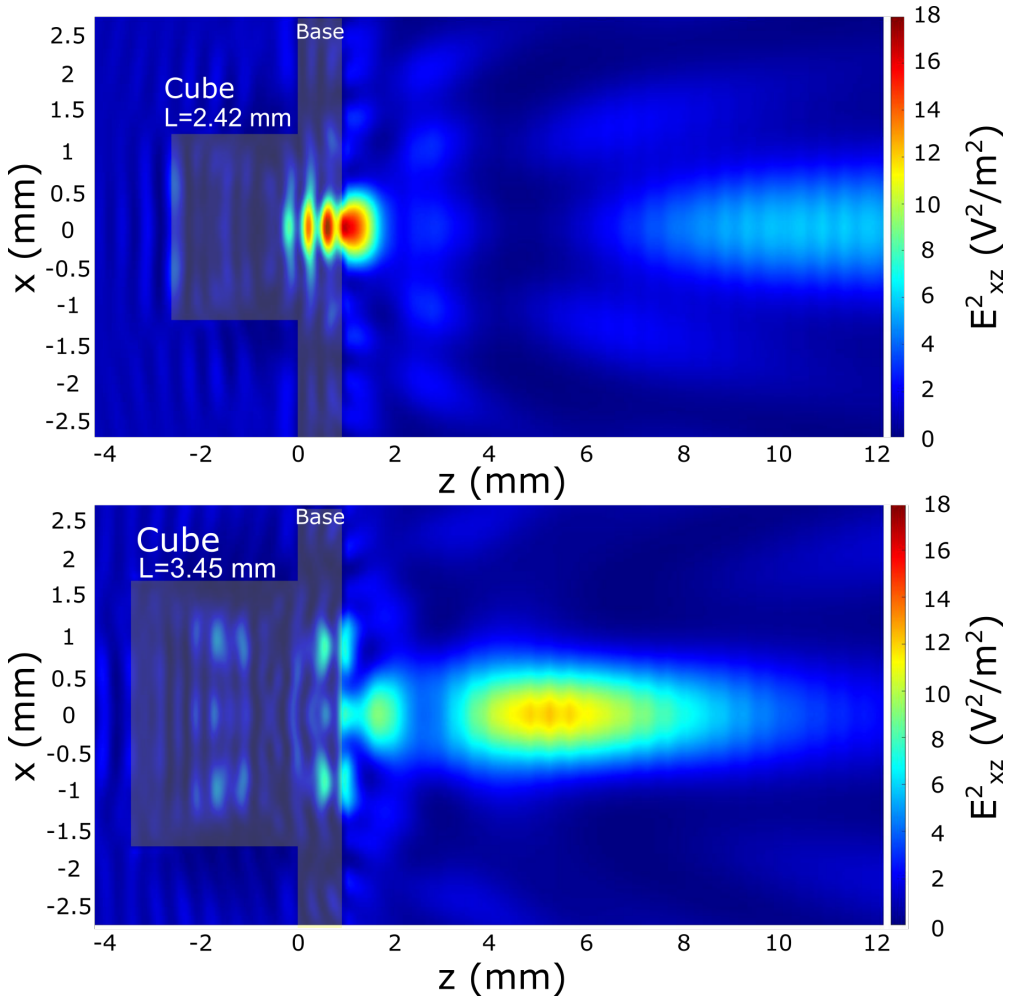

FIG. 4. Intensity of the Electric field in the xz plan (E^2_{xz}) for the case of the cube with edges L=2.42mm (upper plot)and L=3.45mm (lower plot). The cube and it's base are highlighted.

Figure 5 shows the obtained gain (red squares) and the beam focus distance of the terajet beam (blue circles)[37] versus the cube's edge length. The overall behavior is in good agreement with the experimental ones as the introduction of the mesoscopic Teflon cube enhances the gain of the response of the detector due to the terajet effect. The gain reaches a maximum of $\sim$ 13 dB for the cube with L=2.5mm, this value is higher than the one obtained experimentally ($\sim$ 8dB). The reason for this difference is that the focal distance of the terajet for this cube is around 0.65 mm, this means that the focus is placed inside the Teflon base and, therefore, it is not measurable. However, a secondary peak with an intensity considerably lower than the one obtained on the first

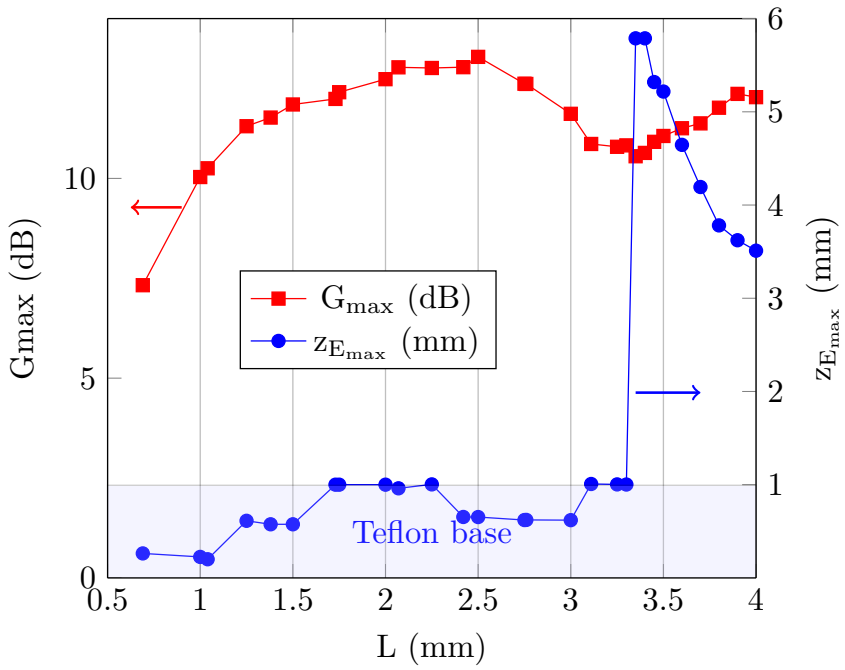

FIG. 5. Maximum gain G_{max} (left axis) and the focal distance ($z_{E_{max}}$) as a function of L.

focus (Figure 4) is measured. However, when considering the cube with L=3.45mm, a maximum gain with a value of $\sim$ 12dB was measured, in excellent agreement with simulations; in this case, as its focal distance is placed at z$\sim$5mm, i.e. outside the Teflon base, measurements were done at the primary maximum of the focal distance. Hence, the position of the focal distance inside or outside the base will condition the values found in measurements and it can explain the behavior of the experimental results when L is varied. Accordingly, the fact the maximum gain was obtained for the cube with the size of 3.45 mm instead of the one with L=2.45mm is justified.

IV. CONCLUSIONS

We report on the enhancement of the responsivity of a plasma-wave FET detector by about 11dB when a mesoscopic dielectric particle was placed in the focal point of a terahertz beam in front of the detector. Several mesoscopic particles (Teflon cubes) with different edge sizes were fabricated and characterized at 0.3THz. The detector exhibit a maximum responsivity of $\sim$ 74 V/W when a cube with an edge size of 3.45mm (3.45λ, where λ is the wavelength of illuminating wave) was placed in the focal position in front of the detector. Full-wave electromagnetic simulations were carried to demonstrate that the terajet effect was the physical mechanism responsible for the

detection enhancement the effect of the terajet as the physical mechanism of the enhancement. This study presents a real solution to enhance the sensitivity of THz detectors though the use of the terajet effect. It's an easy to implement and uncostly solution that can be of benefit to different terahertz applications like inspection and imaging.

ACKNOWLEDGEMENTS

This work was partially conducted within the framework of the Tomsk Polytechnic University Competitiveness Enhancement Program. This research was funded by the Ministerio de Ciencia, Innovación y Universidades of Spain (Spanish Ministry of Science, Innovation, and Universities) and FEDER (ERDF: European Regional Development Fund) under the Research Grants numbers RTI2018-097180-B-100, PID2019-107885GB-C3-2 and TEC2016-78028-C3-3-P and FEDER/Junta de Castilla y León Research Grant numbers SA256P18 and SA121P20 and also by Conselleria d'Educació, lnvestigació, Cultura i Esport, Generalitat Valenciana (Spain) through the grant AIC0/2019/018. This work was supported by "Center for Terahertz Research and Applications (CENTERA)" project, carried out within the 'International Research Agendas' programme of the Foundation for Polish Science co-financed by the European Union under the European Regional Development Fund (no. MAB/2018/9).

CONFLICT OF INTEREST

The authors declare no conflict of interest.

SUPPLEMENTARY MATERIALS

See Supplementary materials file for additional information about the design and fabrication of the Teflon cubes and the DC characteristics of the THz detector.

DATA AVAILABILITY

The data that support the findings of this study are available from the corresponding author upon reasonable request.

REFERENCES

[1]C. Sirtori, "Bridge for the terahertz gap," Nature **417**, 132–133 (2002).

[2]D. Dragoman and M. Dragoman, "Terahertz fields and applications," Progress in Quantum Electronics **28**, 1 – 66 (2004).

[3]D. M. Mittleman, "Perspective: Terahertz science and technology," Journal of Applied Physics **122**, 230901 (2017), https://doi.org/10.1063/1.5007683.

[4]A. Stöhr, "Integrated Microwave-Photonics (iMWP) for Mobile Terahertz Systems," Proc. 43rd International Conference on Infrared, Millimeter, and Terahertz Waves, 9-14 Sept. 2018, Nagoya, Japan (2018), 10.1109/IRMMW-THz.2018.8510119.

[5]K. Ahi, N. Jessurun, M.-P. Hosseini, and N. Asadizanjani, "Survey of terahertz photonics and biophotonics," Opt. Eng. **59**, 061629 (2020).

[6]Y. Tao, A. Fitzgerald, and V. Wallace, "Non-contact, non-destructive testing in various industrial sectors with terahertz technology," Sensors **20(3)**, 712 (2020).

[7]R. A. Lewis, "A review of terahertz detectors," Journal of Physics D: Applied Physics **52**, 433001 (2019).

[8]Y. Meziani, E. Garcìa-Garcìa, J. Velázquez-Pérez, D. Coquillat, N. Dyakonova, W. Knap, I. Grigelionis, and K. Fobelets, "Terahertz imaging using strained-Si MODFETs as sensors," Solid-State Electronics **83**, 113–117 (2013).

[9]S. Kasjoo, M. B. Mohd Mokhar, N. Zakaria, and N. Juhari, "A brief overview of detectors used for terahertz imaging systems," AIP Conference Proceedings **2003**, 020020 (2020).

[10]K. Szkudlarek, M. Sypek, G. Cywiński, J. Suszek, P. Zagrajek, A. Feduniewicz-Żmuda, I. Yahniuk, S. Yatsunenko, A. Nowakowska-Siwińska, D. Coquillat, D. B. But, M. Rachoń, K. Wegrzyńska, C. Skierbiszewski, and W. Knap, "Terahertz 3d printed diffractive lens matrices for field-effect transistor detector focal plane arrays," Opt. Express **24**, 20119–20131 (2016).

[11]J. Grzyb and U. Pfeiffer, "THz Direct Detector and Heterodyne Receiver Arrays in Silicon Nanoscale Technologies," J Infrared Milli Terahz Waves **36**, 998–1032 (2015).

[12]M. Sakhno, J. Gumenjuk-Sichevska, and F. Sizov, "Modeling of the Substrate Influence on Multielement THz Detector Operation," J Infrared Milli Terahz Waves **35**, 703–719 (2014).

[13]S. Zhang, A. Soibel, S. Keo, D. Wilson, S. B. Rafol, D. Ting, A. She, S. Gunapala, and F. Capasso, "Solid-immersion metalenses for infrared focal plane arrays," APL **113**, 111104 (2018).

[14]C. Liu, L. Du, W. Tang, J. Li, L. Wang, G. Chen, X. Chen, and W. Lu, "Towards sensitive terahertz detection via thermoelectric manipulation using graphene transistors," NPG Asia Mater **10**, 318–327 (2018).

[15]Y. Takida, S. Suzuki, M. Asada, and H. Minamide, "Sensitive terahertz-wave detector responses originated by negative differential conductance of resonant-tunneling-diode oscillator," Appl. Phys. Lett. **117**, 021107 (2020).

[16]A. Halpin, W. Cui, A. W. Schiff-Kearn, K. M. Awan, K. Dolgaleva, and J.-M. Ménard, "Enhanced terahertz detection efficiency via grating-assisted noncollinear electro-optic sampling," Phys. Rev. Applied **12**, 031003 (2019).

[17]A. Paulish, A. Gusachenko, A. Morozov, K. Dorozhkin, V. Suslyaev, V. Golyashov, O. V. Minin, and I. V. Minin, "Characterization of tetraaminediphenyl based pyroelectric detector from the visible to millimeter-wave ranges," Optical Engineering **59(6)**, 061612 (2020).

[18]D. Turan, N. Yardinci, and M. Jarrahi, "Plasmonics-enhanced photoconductive terahertz detector pumped by ytterbium-doped fiber laser," Opt. Express **28(3)**, 3835–3845 (2020).

[19]V. Pacheco-Peña, M. Beruete, I. V. Minin, and O. V. Minin, "Multifrequency focusing and wide angular scanning of terajets," Optics Letters **40(2)**, 245–248 (2015).

[20]I. V. Minin and O. V. Minin, "Terahertz artificial dielectric cuboid lens on substrate for super-resolution images," Opt Quant Electron **49**, 326 (2017).

[21]L. Yue, B. Yang, J. Monks, W. Z., N. Tung, V. Lam, O. V. Minin, and I. V. Minin, "A millimetre-wave cuboid solid immersion lens with intensity-enhanced amplitude mask apodization," Journal of Infrared, Millimeter, and Terahertz Waves **39(6)**, 546–552 (2018).

[22]N. Chernomyrdin, A. Kucheryavenko, G. Kolontaeva, G. Katyba, P. Karalkin, V. Parfenov, A. Gryadunova, N. Norkin, O. Smolyanskaya, O. V. Minin, I. V. Minin, V. Karasik, and K. Zaytsev, "A potential of terahertz solid immersion microscopy for visualizing sub-wavelength-scale tissue spheroids," Proc. SPIE 10677, Unconventional Optical Imaging **106771Y** (2018), 10.1117/12.2306132.

[23]N. Pham, S. Hisatake, O. V. Minin, T. Nagatsuma, and I. V. Minin, "Enhancement of spatial resolution of terahertz imaging systems based on terajet generation by dielectric cube," APL Photonics **2**, 056106 (2017).

[24]I. V. Minin, O. V. Minin, J. A. Delgado-Notario, J. Calvo-Gallego, J. E. Velázquez-Pérez, M. Ferrando-Bataller, and Y. M. Meziani, "Improvement of a Terahertz Detector Performance Using the Terajet Effect in a Mesoscale Dielectric Cube: Proof of Concept," physica status solidi

(RRL) - Rapid Research Letters **14**, 1900700 (2020).

[25]O. V. Minin, I. V. Minin, Y. M. Meziani, and S. Hisatake, "Improvement of a point-contact detector performance using the terajet effect initiated by photonics," Optical Engineering **60**, 082004 (2020).

[26]F. D'Angelo, Z. Mics, M. Bonn, and D. Turchinovic, "Ultra-broadband THz time-domain spectroscopy of common polymers using THz air photonics," Optics Express **22**, 12475 (2014).

[27]Y.-S. Jin, G.-J. Kim, and S.-G. Jeon, "Terahertz Dielectric Properties of Polymers," Journal of the Korean Physical Society **49**, 513–517 (2006).

[28]A. Yamaguchi, H. Saito, M. Shimizu, H. Miyajima, S. Matsumoto, Y. Nakamura, and A. Hirohata, "A silicon metal-oxide-semiconductor field-effect transistor hall bar for scanning hall probe microscopy," Rev Sci Instrum. **79(8)**, 083703 (2008).

[29]W. Knap, M. Dyakonov, D. Coquillat, F. Teppe, N. Dyakonova, J. Lusakowski, K. Karpierz, M. Sakowicz, G. Valusis, D. Seliuta, I. Kasalynas, A. El Fatimy, Y. M. Meziani, and T. Otsuji, "Field Effect Transistors for Terahertz Detection: Physics and First Imaging Applications," Journal of Infrared, Millimeter, and Terahertz Waves **30**, 1319–1337 (2009).

[30]J. A. Delgado-Notario, E. Javadi, J. Calvo-Gallego, E. Diez, Y. M. Meziani, J. E. Velázquez-Pérez, and K. Fobelets, "Sub-THz Response of Strained-Silicon MODFETs," physica status solidi (a) **83**, 1700475–6 (2017).

[31]J. A. Delgado-Notario, J. E. Velazquez-Perez, Y. M. Meziani, and K. Fobelets, "Sub-THz Imaging Using Non-Resonant HEMT Detectors," Sensors **18**, 543 (2018).

[32]C.-S. Yang, C.-M. Chang, P.-H. Chen, P. Yu, and C.-L. Pan, "Broadband terahertz conductivity and optical transmission of indium-tin-oxide (ITO) nanomaterials," Optics Express **21**, 16670–16682 (2013).

[33]C. A. Balanis, *Antenna Theory*, Analysis and Design (John Wiley & Sons, 2016).

[34]C. M. O'Sullivan and J. A. Murphy, *Noise Equivalent Power*, Field Guide to Terahertz Sources, Detectors, and Optics (SPIE, 2012).

[35]R. Kokkoniemi, J. Govenius, V. Vesterinen, R. E. Lake, A. M. Gunyhó, K. Y. Tan, S. Simbierowicz, L. Grönberg, J. Lehtinen, M. Prunnila, J. Hassel, A. Lamminen, O.-P. Saira, and M. Möttönen, "Nanobolometer with ultralow noise equivalent power," Communications Physics **2**, 124 (2019).

[36]CST Software: https://www.3ds.com/products-services/simulia/products/cst-studio-suite/.

[37]W. Houston, "A compound interferometer for fine structure work," Phys Rev **29**, 0478–0484 (1927).